

# Optical and dielectrical characteristics of NaCl:Ni<sup>2+</sup> crystals

D. NOWAK-WOŹNY, M. SUSZYŃSKA, M. SZMIDA

*W. Trzebiatowski-Institute of Low Temperature and Structure Research, Polish Academy of Sciences, Wrocław, Poland*

R. CAPELLETTI

*Physics Department, Parma University, Parma, Italy*

Within the spectral ultraviolet range, the optical absorption of NaCl:Ni<sup>2+</sup> crystals exhibits two fairly strong bands and two satellites to the low-energy band. All bands are characteristic of octahedrally surrounded Ni<sup>2+</sup> ions and are related to charge transfer transitions. Two bands, appearing in the ionic thermocurrent spectrum of solution-treated samples, correspond to isolated impurity–vacancy dipoles and the Maxwell–Wagner–Sillars (MWS) polarizations originating in dislocation lines surrounded by Cottrell-like atmospheres. Because of the low thermal stability of dipoles, in as-received samples, only the MWS band is present.

## 1. Introduction

Because of the positive charge excess related to divalent cations (Me<sup>2+</sup>), either one or two cation vacancies are introduced into the monovalent alkali halides (AH). This difference is related to the location of impurities within the crystal lattice, where either substitutional or interstitial positions, respectively, have to be considered. Both types of impurity–vacancy (I–V) complexes are endowed with an electrical dipole moment, the magnitude of which is given by the electronic charge times the geometrical distance between their components. The reorientation of these dipoles, whenever thermally activated, can be monitored by means of the ionic thermocurrent (ITC) technique.

Although energy considerations seem to favour the substitutional location of Me<sup>2+</sup> ions in the AH crystals, an off-centre displacement of the impurities has been found in beryllium-doped NaCl and KCl crystals [1]. For the off-centre based dipoles, a low energy barrier between the impurity and vacancy must be expected as well as a dipole moment smaller than in the case of centrally positioned impurities.

It should be noted that the relaxation phenomena have been little studied for crystal systems in which the size of the dopant,  $r_{2+}$ , is distinctly smaller than the size of the matrix cation,  $r_+$ . In spite of an interest in such studies (both in the experiments and the theory as well), parallel measurements of thermally stimulated depolarization currents (ITC) and the optical absorption (OA) have been performed for NaCl:Ni<sup>2+</sup> crystals of different origins. Both characteristics of these crystals have been investigated [2–7]. There are, however, some differences which are probably related to the crystal growth conditions. On the other hand, some of the data are reported for the first time; first and foremost, an effort to understand the clustering of impurities should be mentioned.

## 2. Experimental procedure

The NaCl:Ni<sup>2+</sup> crystals have been either grown in our laboratory or purchased from the Laboratories mentioned in Table I. Some modifications of the Bridgman method were brought about in order to minimize the contamination by oxygen-containing anions. The dopant concentration,  $c_{2+}$ , was determined by both the atomic absorption analysis as well as the optical absorption measurements. In the latter case a calibration curve of the form  $c_{2+}[\text{mole p.p.m.}] = A\alpha^c$  was exploited; the calibration factor,  $A$ , equals 1.78 for the absorption coefficient,  $\alpha^c$ , ( $\text{cm}^{-1}$ ) [8]. Optical absorption data have been taken at room temperature within the spectral range  $195 \text{ nm} \leq \lambda \leq 333 \text{ nm}$  by using the Specord (Zeiss) M-40 spectrophotometer.

For ITC measurements the procedure developed by Bucci *et al.* [9] was employed in an extended (LNT–393 K) temperature range. The polarization current  $i$  was detected by a vibrating reed electrometer (Cary 31 V) and recorded by Speedomax; currents as low as  $10^{-16}$  A were measured.

The solution treatment (ST) of as-received (AR) samples comprised 30 min annealing at about 873 K

TABLE I Basic characteristics of the crystals

Sample	Origin	$c_{2+}$ (mp.p.m.)	
		Melt	Sample (by AAS)
T.5	Research Laboratory of	$10^2$	Not made
T.2.1	Crystal Physics,	$3 \times 10^2$	Not made
T.2.3	HAS, Budapest		40
T.1.7	Institute of Physics, SAS, Bratislava	$10^3$	64
T.6.0	Our laboratory	$10^3$	Not made
T.6.1			178
T.6.4			55

and the air-quenching to room temperature (RT). Additional measurements have been performed for ST samples aged at 293, 343 and 573 K.

### 3. Results and discussion

#### 3.1. Optical absorption

##### 3.1.1. AR and ST data

Fig. 1a–d shows the OA spectra taken at RT for AR, ST and two additionally annealed samples, respectively, whereas Table II collects some numerical data. The main features of these absorptions are summarized below.

1. The spectra are dependent on both the dopant concentration and the thermal pretreatment of samples. Some differences relate to the number of bands, to the band amplitude,  $\alpha$  ( $\text{cm}^{-1}$ ), and to the position,  $\lambda$  (nm) of their maxima.

2. The main band (C) appearing at 246 nm is probably not an elementary one, cf. the changes in  $\lambda$  induced by the dopant concentration and also the thermal pretreatment.

3. In contrast to ST samples which show exclusively the presence of bands A and C (cf. Fig. 1), all AR samples exhibit an additional band (B) peaking at about 220 nm and a broad absorption on the long-

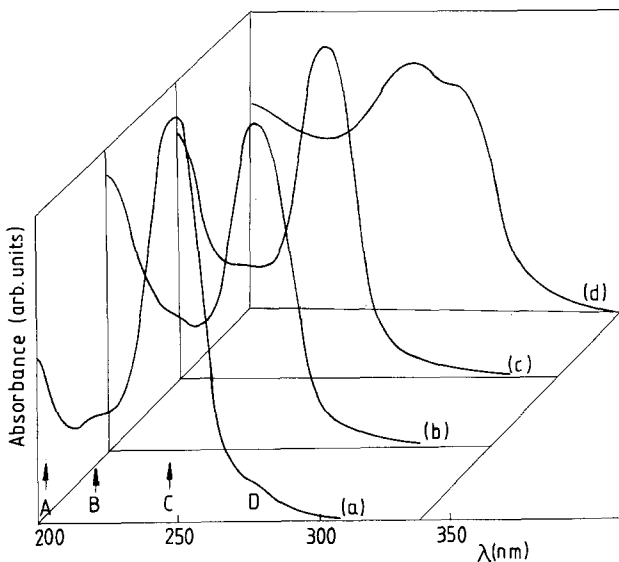


Figure 1 Optical absorption spectra of heavily doped NaCl:  $\text{Ni}^{2+}$  crystals;  $c_{2+} = 178$  mp.p.m. (a) AR, (b) ST and (c, d) two additionally annealed ( $T_{\text{an}} = 343$  and 573 K) samples.

TABLE II Review of the optical data

Sample	$\lambda$ (nm)			
	AR	ST	ST + 343 K	ST + 573 K
T.6.4.	195 (200)	200 –	195 (220)	200 –
	245	248	245	250
	–	–	–	269.5
T.6.1.	195	200	195	200
	220	–	(220)	–
	243	247	244	250
	–	–	–	269

wavelength side of band C; in heavily doped samples this broadening transforms into a distinct D band.

4. The storage of ST samples at room temperature results in a partial recovery of both the intensity and position of the main bands detected. The low-energy satellite of band C, however, appears only in heavily doped samples slowly cooled to room temperature after the annealing at 873 K.

##### 3.1.2. Some annealing effects

Fig. 1. curves c and d were obtained for heavily doped samples additionally annealed at 343 and 573 K and air-quenched to room temperature. These data are representative for a low ( $\text{RT} \leq T_{\text{an}} \leq 473$  K) and high ( $473 \text{ K} \leq T_{\text{an}} \leq 673$  K) temperature annealing range.

It has been stated that after annealings at  $T_{\text{an}} \leq 473$  K the OA spectra are more or less similar to those typical of AR samples, and distinct OA-changes take place after annealings at high temperatures, only; cf. the consecutive changes of band C into a double one. Although the growth of the low-energy component occurs at the expense of the shifted C band, the entire area beneath the absorption outline remains constant during this transformation.

##### 3.1.3. Impurity-related absorption centres

Taking into account the main features of the detected OA spectra, it is assumed that the ultraviolet bands are related to octahedrally coordinated  $\text{Ni}^{2+}$  ions. The local symmetry of these ions in the NaCl crystals studied should correspond to a distorted octahedron, where the distortion results mainly from the charge compensation mechanism. The C band relates with the presence of isolated I–V dipoles as well as simple dipole-aggregates, whereas the centres related to the double absorption band should correspond to mutually penetrable aggregates and/or precipitates rich in vacancies. In favour of this hypothesis are the results of thermally induced density changes reported by Andreev *et al.* [10]. The authors have shown that in the high-temperature annealing range,  $\text{NiCl}_2$  particles are formed with some vacancy–voids included. The precipitation of “pure”  $\text{NiCl}_2$  particles should occur either in the freshly grown crystals or in ST samples additionally annealed at  $T_{\text{an}} \geq 673$  K and slowly cooled to room temperature.

### 3.2. Depolarization phenomena

#### 3.2.1. Some previous data

According to our knowledge there are three publications reporting the relaxation effects in  $\text{Ni}^{2+}$ -doped NaCl crystals. From among the results obtained the following findings merit our attention.

1. ITC spectra of AR samples cut from Bridgman crystals in the form of parallelepipeds exhibit the presence of a huge high-temperature ( $T_m \gg \text{RT}$ ) band, only [11–13]. These polarizations are explainable in frames of the Maxwell–Wagner–Sillars theory for polarizations in heterogeneous dielectrics, whereby dislocation lines surrounded by impurities play the role of polarizable entities.

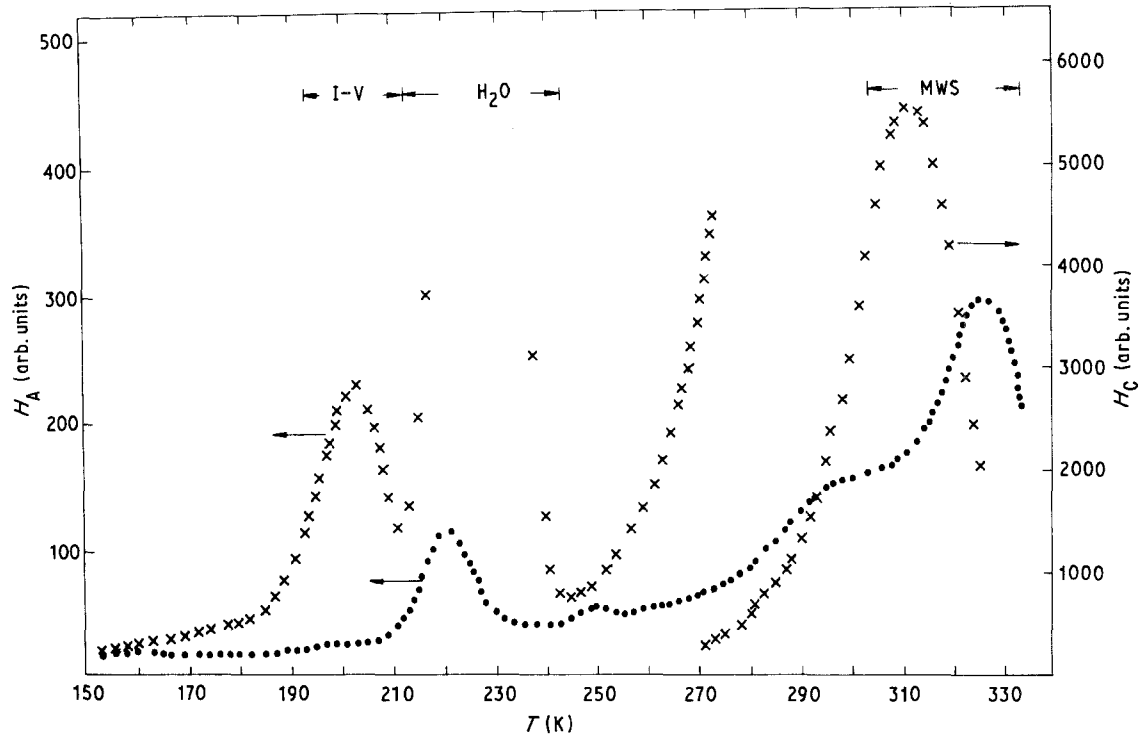


Figure 2 ITC spectra for plate-shaped T.6.0 samples;  $E_p \cong 7.5 \text{ kV cm}^{-1}$ ,  $T_p \cong \text{RT}$ ,  $T_f \cong \text{LNT}$ ,  $t_p = 3 \text{ min}$ . (●) AR and (×) ST samples

2. For Czochralski crystals [7] the small ITC dipole-band is accompanied by a huge, broad band located near room temperature. The origin of this band was tentatively ascribed to the Suzuki phase coexisting with isolated dipoles.

3. The dielectric losses, measured for Kyropoulos crystals [2, 3], show the presence of a single band at 310 K, which disappears after about 50 days ageing at room temperature.

### 3.2.2. AR and ST data

The ITC spectra obtained for plate-shaped samples (cut from crystals of different origin) at liquid nitrogen temperature ( $\text{LNT}) \leq T_{\text{test}} \leq 373 \text{ K}$  are qualitatively similar to each other. In contrast to the Czochralski crystals [7] the so-called Suzuki-band was not detected. Fig. 2 shows some ITC spectra of variously treated samples, and Table III collects the main features of the bands detected. It has been stated that in as-received samples the dipole band (located at 203 K) is very small and its shape does not depend on the

dopant concentration and the thermal pretreatment of samples. The band intensity,  $H^A$ , increases with  $c_{2+}$  and the solution treatment. In order to avoid some overlapping with  $\text{H}_2\text{O}$  relaxations, the samples were polarized at  $T_p \leq 238 \text{ K}$ . The linearity of  $H^A$  with the polarization field,  $E_p$ , and the relatively weak polarization of this band, are consistent with dielectric relaxations induced by a low concentration of non-interacting dipoles.

There is no reason to assume that all nickel ions are in the form of isolated I-V dipoles and that all dipoles are of one type, only. Table III collects the concentrations of dipoles, calculated according to Bucci *et al.* [9], for the *nn*-configuration. The comparison of these values with  $c_{2+}$  clearly shows that only a part of the dopant is in the form of isolated dipoles. Although the small  $\text{Ni}^{2+}$  ions should prefer the formation of *nnn*-dipoles, see, for instance, Fig. 24 in [14], the problem of “*nn*- or *nnn*-configuration” will remain open for this series of data. Table III also gives the values of the reorientation activation energy,  $E_i$  and the frequency factor,  $\tau_0^{-1}$ . Estimation of  $E_i$  was made according to Chen’s approximations for the first-order kinetics [15], whereas  $\tau_0$  was calculated from the condition for the band maximum, (see [9]). It should be noted that the value of  $E_i$  obtained is in the range expected for a small impurity ion, see, for instance, Table 3.6. in Reference 16, and agrees well with the value obtained previously [7].

### 3.2.3. Storage at room temperature

Over the course of several days at room temperature, the amplitude of the dipole band decreases considerably, i.e. the dipoles transform into some clusters which no longer contribute to the ITC band. During this process no other ITC band grows. Fig. 3 shows

TABLE III Main features of the ITC spectrum

Sample	$c_{2+}$ by OA	Thermal history	$T_m^c(\text{K})$	$c_{IV}$ for <i>nn</i>	Remarks
T.5.	4.5	AR	330	0.0	$E_i = 0.55 \text{ eV}$
		ST	319	6.0	$\tau_0 = 8.26 \times 10^{-13} \text{ s}$
T.2.1.	10.4	AR	322	1.1	$T_p \cong \text{RT}; T_f \cong \text{LNT}$
		ST	314	6.7	$t_p = 3 \text{ min}$
T.2.3.	38.2	AR	329	0.9	$V_p \cong 950 \text{ V}$
		ST	310	24.0	
T.1.7.	73.3	AR	334	2.5	
		ST	314	38.0	
T.6.0.	$\gg 180$	AR	325	0.6	
		ST	310	103.0	

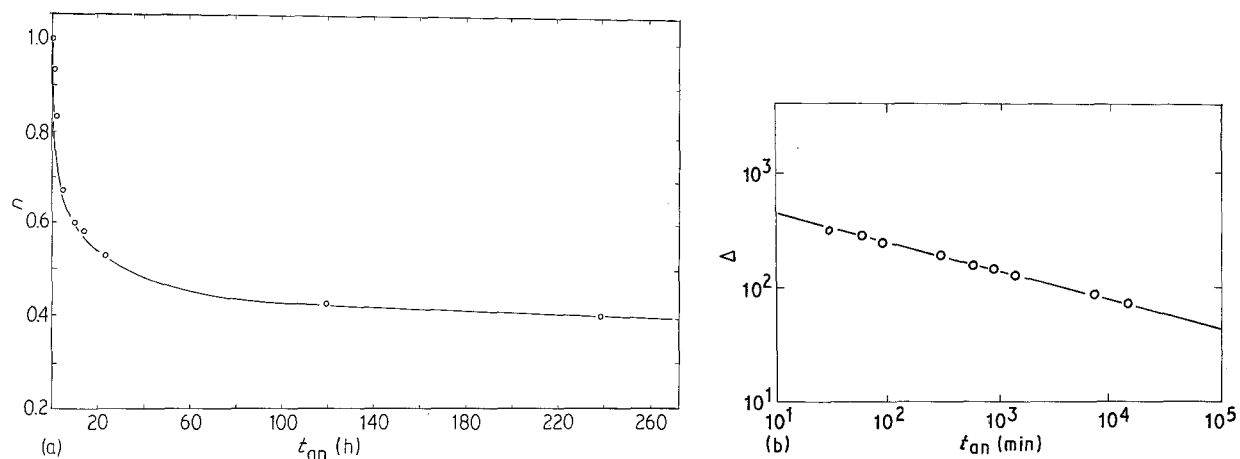


Figure 3 (a) Fractional dipole concentration versus annealing time at RT for a solution-treated T.6.0. sample. (b) A log-log plot of  $\Delta [ \equiv n(t_{an}) - n(\infty) ]$  versus  $t_{an}$ .

the concentration of dipoles  $n(t_{an})$  normalized to the initial value of  $n(ST)$  versus annealing time  $t_{an}$  at room temperature. The decomposition is probably a two-stage process with a saturation after about 62.5 % of the dipoles have disappeared. The best fitting of the experimental results was obtained for the drift of impurities towards dislocations, cf. the Cottrell/Bilby approach [17]. The degree of supersaturation  $\Delta = [n(t_{an}) - n(\infty)]$  falls like  $t_{an}^{-m}$  with  $m = 0.26$ , see Fig.3b;  $n(\infty)$  denotes the saturation concentration of dipoles. The special role of dislocations in the aggregation/precipitation processes should be confirmed for plastically deformed samples, for instance.

#### 4. Conclusion

By comparing the optical and dielectric characteristics of NaCl:Ni<sup>2+</sup> crystals, the following conclusions could be drawn. The optical spectrum arises from electronic transitions localized either at isolated I-V dipoles and small dipole aggregates (in solution-treated samples) or at larger aggregates and second-phase particles in as-received and thermally pretreated solution-treated samples). Because the presence and/or formation of the Suzuki phase and a mixed salt (such as NaNiCl<sub>3</sub>) have not been confirmed, we suggest that NiCl<sub>2</sub> particles without and with some vacancy voids included, determine the properties of as-received and also annealed solution-treated samples, respectively. Preliminary measurements of the yield strength of the NaCl:Ni<sup>2+</sup> crystals are in favour of this suggestion.

#### Acknowledgements

The work was performed in frames of the Scientific

Cooperation Agreement between the Polish Academy of Sciences and the Consiglio Nazionale Delle Ricerche (Italy). One of us (M. Suszyńska) acknowledges the hospitality of the Physics Department of Parma University, Italy, where the ITC spectra were measured.

#### References

1. C. BUCCI, *Phys. Rev.* **164** (1967) 1200.
2. M. KADERKA, *Czech. J. Phys. B* **18** (1968) 1222.
3. *Idem, ibid.* **19** (1969) 530.
4. T. NASU and Y. ASANO, *J. Phys. Soc. Jpn* **27** (1969) 264.
5. K. POLAK, *Z. Physik* **223** (1969) 338.
6. R. VOSZKA, A. WATTERICH, I. FÖLDVARI, A. BOHUN and K. POLAK, *Czech. J. Phys. B* **23** (1973) 670.
7. G. BENEDEK, J. M. CALLEJA, R. CAPELLETTI and A. BREITSCHWERDT, *J. Phys. Chem. Solids* **45** (1984) 741.
8. D. NOWAK-WOŹNY and M. SUSZYŃSKA, *Acta. Phys. Polon. A* **81** (1992) 419.
9. C. BUCCI, R. FIESCHI and G. GUIDI, *Phys. Rev.* **148** (1966) 816.
10. G. A. ANDREEV, M. HARTMANOVÁ and V. A. KLIMOV, *Phys. Status Solidi (a)* **41** (1977) 679.
11. M. SUSZYŃSKA and R. CAPELLETTI, *Crystal Res. Technol.* **19** (1984) 1385.
12. *Idem, ibid.* **19** (1984) 1484.
13. *Idem, ibid.* **20** (1985) 1363.
14. F. AGULLO-LOPEZ, J. M. CALLEJA, F. CUSSO, E. JAQUE and F. J. LOPEZ, *Prog. Mater. Sci.* **30** (1986) 187.
15. R. CHEN, *J. Appl. Phys.* **40** (1969) 570.
16. J. VAN TURNHOUT, "Topics in Applied Physics", vol. 33, edited by G. M. Sessler (Springer, Berlin, 1980).
17. A. H. COTTRELL and A. B. BILBY, *Proc. Phys. Soc. A* **62** (1949) 49.

Received 19 July 1991

and accepted 11 March 1992